TOTAL CROSS-SECTION AT LHC FROM MINIJETS AND SOFT GLUON RESUMMATION IN THE INFRARED REGION*

G. Pancheri

INFN Frascati National Laboratories, P.O. Box 13, I00044 Frascati, Italy

R.M. Godbole

Centre for High Energy Physics, Indian Institute of Science
Bangalore, 560 012, India

A. Grau

Departamento de Física Teórica y del Cosmos, Universidad de Granada, Spain

Y.N. Srivastava

Physics Department and INFN, University of Perugia, Perugia, Italy

(Received June 28, 2007)

A model for total cross-sections incorporating QCD jet cross-sections and soft gluon resummation is described and compared with present data on pp and $\bar{p}p$ cross-sections. Predictions for LHC are presented for different parameter sets. It is shown that they differ according to the small x-behaviour of available parton density functions.

PACS numbers: 12.38.–t, 12.40.Nn, 13.60.Hb, 13.85.Lg

1. Introduction

The upcoming measurements at LHC are renewing considerable interest regarding predictions for total cross-sections. The model [1, 2] we shall describe in the following, attempts to link the rate with which total cross-sections rise, to the infrared behaviour of the strong coupling constant α_s

* Presented at The Final EURIDICE Meeting "Effective Theories of Colours and Flavours: from EURODAPHNE to EURIDICE", Kazimierz, Poland, 24–27 August, 2006.

and to QCD hard parton–parton scattering, using known phenomenological entities such as the available QCD parton density functions (PDFs).

2. The model

The energy behaviour of the total cross-section exhibits the following properties [3]

- an initial decrease;
- a sharp change in curvature occurring somewhere between 20 and 50 GeV in the c.m. of the scattering hadrons;
- a smooth rise which asymptotically follows a $\ln s$ or $\ln^2 s$ type increase in consonance with the Froissart bound [4, 5].

The model we use is based on

1. hard component of scattering responsible for the rise of the total cross-section [6, 7];
2. soft gluon emission from scattering particles which softens the rise [1];
3. eikonal transformation which implies multiple scattering and requires impact parameter distributions inside scattering particles and basic scattering cross-sections [8].

According to our model, soft gluon emission is responsible for the initial decrease in pp, as well as for the transformation of the sharp rise due to the increase in gluon–gluon interactions into a smooth behaviour. Thus soft gluon emission plays a crucial role, with care taken to extend resummation to the zero energy modes, in complete analogy for what is required by the Bloch–Nordsieck theorem for QED [9]. The model can then be referred to as the BN model, for reasons which will also be clearer in the following.

2.1. Details of the BN model

We use the following eikonal expression for the total inelastic cross-section:

$$\sigma_{\text{inel}} = \int d^2\vec{b} \left[1 - e^{-n(b,s)}\right] , \tag{1}$$

where $n(b, s)$ corresponds to the average number of inelastic collisions at any given value of the impact parameter b. Neglecting the real part of the eikonal, we then calculate the total cross-section as

$$\sigma_{\text{total}} = 2 \int d^2\vec{b} \left[1 - e^{-n(b,s)/2}\right] . \tag{2}$$

In our model $n(b,s)$ is split as

$$n(b,s) = n_{\rm soft}(b,s) + n_{\rm hard}(b,s)\,, \tag{3}$$

where we postulate the following factorisation

$$n_{\rm soft/hard}(b,s) = A_{\rm BN}^{\rm soft/hard}(b,s)\sigma_{\rm soft/hard}(s) \tag{4}$$

with

$$A_{\rm BN}(b,s) = N\int d^2K_\perp\ e^{-iK_\perp\cdot b}\frac{d^2P(K_\perp)}{d^2K_\perp}\,, \tag{5}$$

where N is a normalisation factor such that $\int d^2\vec{b}A(b) = 1$ and

$$\frac{d^2P(K_\perp)}{d^2K_\perp} = \frac{1}{(2\pi)^2}\int d^2\vec{b}\ \exp\left\{iK_\perp\cdot b - \int_0^{q_{\rm max}} d^3\bar{n}(k)[1-e^{-ik_{\rm t}\cdot b}]\right\} \tag{6}$$

is the transverse momentum distribution of initial state soft gluons emitted in the parton–parton collisions and where, for simplicity, $k_\perp\cdot b = \vec{k}_\perp\cdot\vec{b}$. In equation (6) $q_{\rm max}$ is the maximum transverse momentum allowed by kinematics to single soft gluon emission in a given hard collision, averaged over the parton densities. According to the basic ansatz of the Eikonal Minijet Model (EMM),

$$\begin{aligned}\sigma_{\rm hard} &\equiv \sigma_{\rm jet}^{AB}(s)\\ &= \int_{p_{\rm tmin}}^{\sqrt{s/2}} dp_{\rm t}\int_{4p_{\rm t}^2/s}^1 dx_1\int_{4p_{\rm t}^2/(x_1s)}^1 dx_2\sum_{i,j,k,l} f_{i|A}(x_1)f_{j|B}(x_2)\ \frac{d\hat{\sigma}_{ij}^{kl}(\hat{s})}{dp_{\rm t}}\,.\end{aligned} \tag{7}$$

Here A and B denote particles ($\gamma,\ p,\ldots$), $i,\ j,\ k,\ l$ are parton types and x_1, x_2 the fractions of the parent particle momentum carried by the parton. $\hat{s} = x_1x_2s$ and $\hat{\sigma}$ are hard parton scattering cross-sections. As discussed in [1], kinematical considerations suggest [10]

$$q_{\rm max}(s) = \frac{\sqrt{s}}{2}\,\frac{\sum_{i,j}\int\frac{dx_1}{x_1}f_{i|A}(x_1)\int\frac{dx_2}{x_2}f_{j|B}(x_2)\sqrt{x_1x_2}\int_{z_{\rm min}}^1 dz(1-z)}{\sum_{i,j}\int\frac{dx_1}{x_1}f_{i|A}(x_1)\int\frac{dx_2}{x_2}f_{j|B}(x_2)\int_{z_{\rm min}}^1(dz)} \tag{8}$$

with $z_{\rm min} = 4p_{\rm tmin}^2/(sx_1x_2)$ and $f_{i/a}$ the valence quark densities used in the jet cross-section calculation. The steps we follow to compare the model with data are then the following:

1. choose the parameters for the hard scattering part, namely
   (*i*) parton densities (PDF), p_{tmin} and Λ_{QCD} for the chosen PDF set in equation (7),
   (*ii*) model for α_{s} in the infrared region and relevant parameters in equation (6),
2. calculate $q_{\mathrm{max}}(s, p_{\mathrm{tmin}})$ for the given densities and p_{tmin} using equation (8),
3. calculate $n_{\mathrm{hard}}(b,s) = A_{\mathrm{BN}}^{\mathrm{hard}}(b,s)\sigma_{\mathrm{jet}}(s, p_{\mathrm{tmin}})$,
4. choose the parameters for the low energy part, namely
   (*i*) the constant low energy cross-section σ_0,
   (*ii*) values for $q_{\mathrm{max}}^{\mathrm{soft}}$,
5. calculate $n_{\mathrm{soft}}(b,s) = A_{\mathrm{BN}}^{\mathrm{soft}}(b,s)\sigma_0(1 + \epsilon\frac{2}{\sqrt{s}})$ with $\epsilon = 0, 1$ depending upon the process being pp or $p\bar{p}$,
6. calculate $n(b,s)$ and thus σ_{tot},
7. choose the parameter set which gives the best description of the total cross-section up to the Tevatron data [11–13].

Notice that once a good set of parameters is found, one can use $n(b,s)$ with fitted parameters to calculate survival probabilities or diffractive Higgs production.

2.2. Application to total cross-section data

We show in this section the application of the model to the total cross-section for different PDFs. We find that our model is flexible enough to be able to reproduce the present data for σ_{tot} using all presently available PDFs. In particular, all GRV [14–16] and MRST [17] densities give a good description using the singular α_{s} model described in [1], while CTEQ densities [18] give an acceptable fit up to Tevatron data, but the cross-section fails to rise further.

We present these results by following the previously listed steps. We start by choosing the parameters for the hard scattering, and, following our previous results [2], we fix $p_{\mathrm{tmin}} = 1.15$ GeV in the jet cross-sections and calculate q_{max} for different PDF sets. We show the result in Fig. 1.

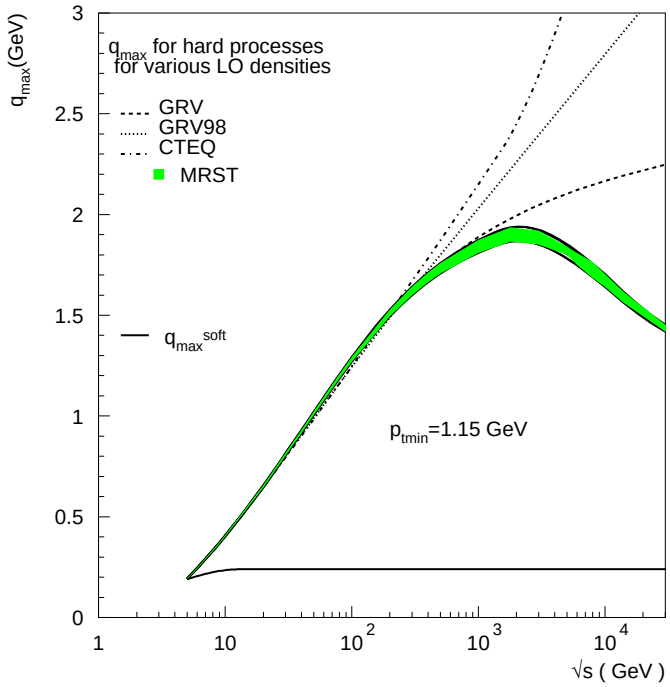

Fig. 1. Average value of the maximum transverse momentum allowed to single gluon emission, according to the model in [2].

We notice the following:

- GRV densities are of two types, GRV98 [16] for which $q_{\max}$ keeps on increasing logarithmically and the older ones [14] for which $q_{\max}$ slows down past the TeV region, albeit still slowly increasing.
- CTEQ densities give values for $q_{\max}$ which increase more rapidly than $\ln s$ after typical Tevatron energies.
- MRST densities indicate a behaviour opposite to CTEQ, since they give $q_{\max}$ values decreasing after the TeV cross mark.

We now turn to the jet cross-sections and examine the growth with energy of $\sigma_{\rm jet}$ for different PDFs. In Fig. 2 we plot these cross-sections for the same set of densities used to calculate $q_{\max}$ and for $p_{\rm tmin} = 1.15$ GeV. From this figure we notice that :

- the jet cross-sections for GRV densities increase faster than all the others;

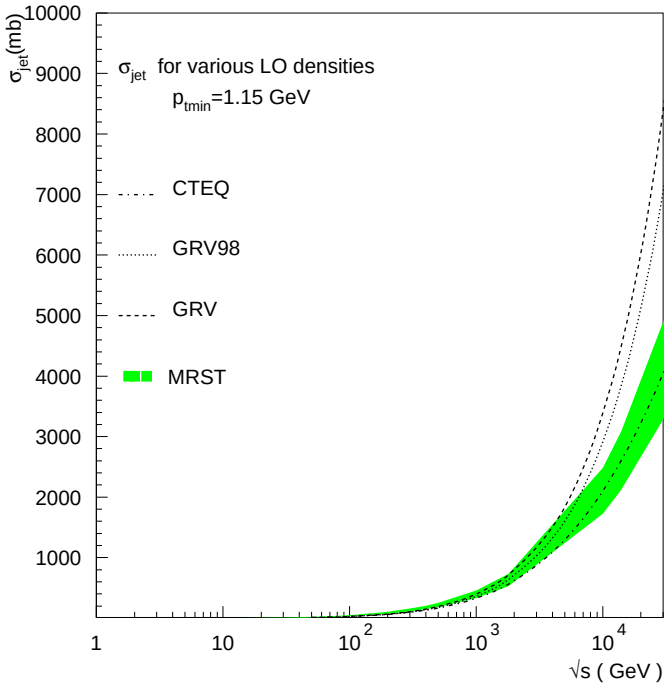

Fig. 2. Mini-jet QCD cross-sections for different PDFs as indicated in the figure.

- the jet cross-sections for CTEQ increase more or less similarly to those for the MRST group.

The implications are that $\sigma_{\rm jet}$ with GRV densities, which increase faster than $\sigma_{\rm jet}$ with MRST, need more softening, $\sigma_{\rm jet}$ with CTEQ, which increase less than with GRV, should not be smeared that much.

To proceed further, we now need to calculate the b-distribution and fix the low-energy parameters, like σ_0. The b-distribution requires to input the behaviour of $\alpha_{\rm s}$ in the infrared region. We have shown in [2] the need to use a singular but integrable expression for $\alpha_{\rm s}$ in order to reproduce both the sudden rise and the subsequent softening of the total cross-section. Our choice is an expression like

$$\alpha_{\rm s}(k_{\rm t}) = \frac{12\pi}{(33-2N_f)} \frac{p}{\ln[1+p(\frac{k_{\rm t}}{\Lambda})^{2p}]} \tag{9}$$

which depends on the singularity parameter p, in addition to the scale Λ. In [2] we have chosen the value $p = 0.75$ and $\Lambda = 100$ MeV, other choices are

also possible [19]. Turning now to the low-energy part, $n_{\rm soft}(b,s)$, we choose $\sigma_0 = 48$ mb and use for $A_{\rm BN}^{\rm soft}$ a set of $q_{\rm max}$ values which reproduce the low energy behaviour, and which appear in Fig. 1.

3. Comparison with data and expectations at LHC densities

We can now input all the above in the eikonal representation for the total cross-section and obtain the results shown in Fig. 3 for the singular $\alpha_{\rm s}$ case and GRV, MRST and CTEQ densities. For the sake of clarity, we only plot curves for pp scattering, referring the reader to [2,19] for the curves for $p\bar{p}$ and for a different parameter set, or for predictions from other models [5, 20–23]. From the figure we see that the calculation with CTEQ densities appears very unlikely. The effect is due to the fact that the jet cross-sections in the CTEQ case do not rise as much as the others while the softening effect is stronger, as it is driven by $q_{\rm max}$, which is strongly increasing for these densities. As a result, the cross-section starts decreasing. Notice that while

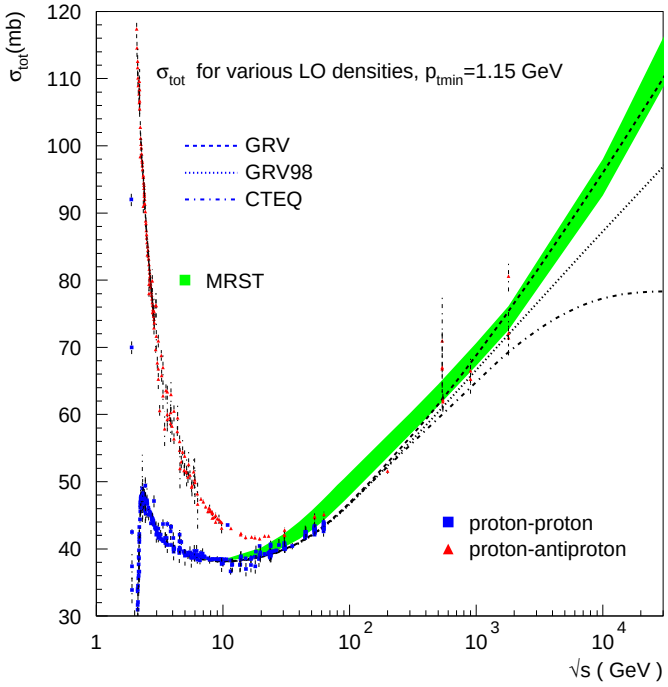

Fig. 3. Data for total cross-sections for pp and $p\bar{p}$ compared with model predictions at LHC for pp scattering, using different PDFs.

the behaviour of $\sigma_{\rm jet}$ is dominated by the gluon densities, that of $q_{\rm max}$ is determined only by the valence quarks, as we assume this to be the leading order effect.

The curves shown in Fig. 3 indicate that the coming measurement at $\sqrt{s} = 900$ GeV will be very important in determining which of these curves best describe the data. It can then be used to select the parameter set, basically PDF's and $p_{\rm tmin}$, for a prediction at the project LHC energy, $\sqrt{s} = 14$ TeV. If the UA5 [24] value at $\sqrt{s} = 900$ GeV is confirmed with a comparable error, then, for the set of parameters discussed in this note, at $\sqrt{s} = 14$ TeV our model gives $\sigma_{\rm total}^{\rm GRV98} = 90.2$ mb, $\sigma_{\rm total}^{\rm GRV} = 100.2$ mb and $\sigma_{\rm total}^{\rm MRST76} = 103.4$ mb. As shown in [19], changing the parameter set, namely σ_0, $p_{\rm tmin}$ or the singularity index p, give values in the range $88 \div 111$ mb.

4. Conclusions

We have presented a version of the eikonal minijet model which allows a good description of total cross-sections at asymptotic energies and discussed its connection with the small x-behaviour of various types of parton densities. This model is based on a softening of the mini-jet cross-sections due to an s-dependent b-distribution in the proton, which we calculate using a soft gluon resummation model down to zero energy of the soft gluons.

We acknowledge partial support from EU CT-2002-0311.

REFERENCES

[1] A. Corsetti, A. Grau, G. Pancheri, Y.N. Srivastava, *Phys. Lett.* **B382**, 282 (1996) [hep-ph/9605314]; A. Grau, G. Pancheri, Y.N. Srivastava, *Phys. Rev.* **D60**, 114020 (1999) [hep-ph/9905228].

[2] R.M. Godbole, A. Grau, G. Pancheri, Y.N. Srivastava, *Phys. Rev.* **D72**, 076001 (2005) [hep-ph/0408355].

[3] Particle Data Group, *J. Phys. G: Nucl. Part. Phys.* **33**, 1 (2006).

[4] M. Froissart, *Phys. Rev.* **123**, 1053 (1961).

[5] M.M. Block, F. Halzen, *Phys. Rev.* **D72**, 036006 (2005), Erratum *Phys. Rev.* **D72**, 039902 (2005) [hep-ph/0506031].

[6] D. Cline, F. Halzen, J. Luthe, *Phys. Rev. Lett.* **31**, 491 (1973); T.K. Gaisser, F. Halzen, *Phys. Rev. Lett.* **54**, 1754 (1985).

[7] G. Pancheri, Y.N. Srivastava, *Phys. Lett.* **B182**, 199 (1986).

[8] L. Durand, P. Hong, *Phys. Rev. Lett.* **58**, 303 (1987).

[9] F. Bloch, A. Nordsieck, *Phys. Rev.* **52**, 54 (1937).

[10] P. Chiappetta, M. Greco, *Nucl. Phys.* **B199**, 77 (1982).

[11] N. Amos *et al.* [E710 Collaboration], *Phys. Rev. Lett.* **68**, 2433 (1992).

[12] F. Abe *et al.* [CDF Collaboration], *Phys. Rev.* **D50**, 5550 (1994).

[13] C. Avila *et al.*, [E811 Collaboration], *Phys. Lett.* **B445**, 419 (1999).

[14] M. Gluck, E. Reya, A. Vogt, *Z. Phys.* **C53**, 127 (1992).

[15] M. Gluck, E. Reya, A. Vogt, *Z. Phys.* **C67**, 433 (1995).

[16] M. Gluck, E. Reya, A. Vogt, *Eur. Phys. J.* **C5**, 461 (1998) [hep-ph/9806404].

[17] A.D. Martin, R.G. Roberts, W.J. Stirling, R.S. Thorne, *Phys. Lett.* **B531**, 216 (2002) [hep-ph/0201127].

[18] H.L. Lai, J. Botts, J. Huston, J.G. Morfin, J.F. Owens, Jian-wei Qiu, W.K. Tung, H. Weerts, *Phys. Rev.* **D51**, 4763 (1995) [hep-ph/941040].

[19] R.M. Godbole, A. Grau, R. Hegde, G. Pancheri, Y. Srivastava, *Pramana* **66**, 657 (2006), [hep-ph/0604214].

[20] A. Donnachie, P.V. Landshoff, *Phys. Lett.* **B296**, 227 (1992) [hep-ph/9209205]; *Phys. Lett.* **B595**, 393 (2004).

[21] M.M. Block, E.M. Gregores, F. Halzen, G. Pancheri, *Phys. Rev.* **D60**, 054024 (1999) [hep-ph/9809403].

[22] J.R. Cudell *et al.* [COMPETE Collaboration], *Phys. Rev. Lett.* **89**, 201801 (2002) [hep-ph/0206172]; J.R. Cudell *et al.*, hep-ph/0212101.

[23] E.G.S. Luna, A.F. Martini, M.J. Menon, A. Mihara, A.A. Natale, *Phys. Rev.* **D72**, 034019 (2005) [hep-ph/0507057]; R.F. Avila, E.G.S. Luna, M.J. Menon, *Phys. Rev.* **D67**, 054020 (2003) [hep-ph/0212234].

[24] G.J. Alner *et al.* [UA5 Collaboration], *Z. Phys.* **C32**, 153 (1986).